

# **ECHOES**

**Extended Calculator of HOmogEnization Schemes**

Jean-François Barthélémy

11/10/22

# Table of contents

<b>Welcome</b>	<b>4</b>
<b>Introduction</b>	<b>5</b>
<b>I    Linear elasticity</b>	<b>6</b>
1    Basic problem	7
2    Eshelby problem	8
3    Cracks	9
4    Morphologically representative patterns	10
5    Homogenization schemes	11
<b>II   Conductivity</b>	<b>12</b>
6    Basic problem	13
7    Eshelby problem	14
8    Cracks	15
9    Morphologically representative patterns	16
10   Homogenization schemes	17
<b>III   Nonlinear homogenization</b>	<b>18</b>
11   Second order moments	19
12   Differentiation of concentration tensors	20
13   Homogenization schemes	21

<b>IV Viscoelasticity in frequency domain</b>	<b>22</b>
14 Basic problem	23
15 Homogenization schemes	24
<b>V Viscoelasticity in time domain</b>	<b>25</b>
16 Basic problem	26
17 Homogenization schemes	27
<b>VI Examples of implementation</b>	<b>28</b>
18 Concrete strength	29
References	30
<b>Appendices</b>	<b>30</b>
<b>A Tensor algebra</b>	<b>31</b>
<b>B Hill polarization tensor in elasticity</b>	<b>32</b>
B.1 General expression . . . . .	32
B.2 Isotropic matrix . . . . .	32
B.3 Case of cracks . . . . .	35
B.4 Application of Hill calculation . . . . .	36
B.4.1 Definition of the matrix tensor . . . . .	36
B.4.2 Calculation of the crack compliance $\mathbb{L} = \lim_{\omega \rightarrow 0} \omega \mathbb{Q}^{-1}$ . . . . .	37
B.4.3 Checking the aspect ratio for which $\omega \mathbb{Q}^{-1} \approx \lim_{\omega \rightarrow 0} \omega \mathbb{Q}^{-1}$ is acceptable	37
<b>C Hill polarization tensor in conductivity</b>	<b>39</b>

# Welcome

The library **ECHOES** allows to implement various homogenization schemes involving different types of heterogeneities in the framework of elasticity, conductivity, viscoelasticity as well as tools to properly calculate the derivatives of macroscopic stiffness with respect to lower scale moduli (fundamental tool of the modified secant method in nonlinear homogenization).

This manual aims at recalling some fundamental aspects of the theory of homogenization of random media along with a presentation of the main features of the library **ECHOES** as well as code examples.

# Introduction

**Part I**

**Linear elasticity**

# 1 Basic problem

## 2 Eshelby problem



## 3 Cracks

## **4 Morphologically representative patterns**

## **5 Homogenization schemes**

## **Part II**

# **Conductivity**

## 6 Basic problem

## 7 Eshelby problem

## 8 Cracks

## **9 Morphologically representative patterns**



## 10 Homogenization schemes

## **Part III**

# **Nonlinear homogenization**

## 11 Second order moments

## **12 Differentiation of concentration tensors**

## **13 Homogenization schemes**

## **Part IV**

# **Viscoelasticity in frequency domain**

## 14 Basic problem

## **15 Homogenization schemes**



## **Part V**

# **Viscoelasticity in time domain**

## 16 Basic problem

## **17 Homogenization schemes**

## **Part VI**

# **Examples of implementation**

## **18 Concrete strength**

# References

- Abramowitz, M., Stegun, I.A., 1972. Handbook of Mathematical Functions. National Bureau of Standards - Applied Mathematics Series - 55, Washington D.C.
- Barthélémy, J.-F., 2020. Simplified approach to the derivation of the relationship between Hill polarization tensors of transformed problems and applications. *International Journal of Engineering Science* 154, 103326. <https://doi.org/10.1016/j.ijengsci.2020.103326>
- Barthélémy, J.-F., 2009. Compliance and Hill polarization tensor of a crack in an anisotropic matrix. *International Journal of Solids and Structures* 46, 4064–4072. <https://doi.org/10.1016/j.ijsolstr.2009.08.003>
- Barthélémy, J.-F., Sevostianov, I., Giraud, A., 2021. Micromechanical modeling of a cracked elliptically orthotropic medium. *International Journal of Engineering Science* 161, 103454. <https://doi.org/10.1016/j.ijengsci.2021.103454>
- Eshelby, J.D., 1957. The determination of the elastic field of an ellipsoidal inclusion, and related problems. *Proceedings of the Royal Society of London. Series A. Mathematical and Physical Sciences* 241, 376–396. <https://doi.org/10.1098/rspa.1957.0133>
- Gavazzi, A.C., Lagoudas, D.C., 1990. On the numerical evaluation of Eshelby's tensor and its application to elastoplastic fibrous composites. *Computational Mechanics* 7, 13–19. <https://doi.org/10.1007/BF00370053>
- Ghahremani, F., 1977. Numerical evaluation of the stresses and strains in ellipsoidal inclusions in an anisotropic elastic material. *Mechanics Research Communications* 4, 89–91. [https://doi.org/10.1016/0093-6413\(77\)90018-0](https://doi.org/10.1016/0093-6413(77)90018-0)
- Kellogg, O.D., 1929. Potential theory. Berlin : Springer-Verlag.
- Masson, R., 2008. New explicit expressions of the Hill polarization tensor for general anisotropic elastic solids. *International Journal of Solids and Structures* 45, 757–769. <https://doi.org/10.1016/j.ijsolstr.2007.08.035>
- Mura, T., 1987. *Micromechanics of Defects in Solids*, Second Edition. Kluwer Academic. <https://doi.org/10.1002/zamm.19890690204>
- Willis, J.R., 1977. Bounds and self-consistent estimates for the overall properties of anisotropic composites. *Journal of the Mechanics and Physics of Solids* 25, 185–202. [https://doi.org/10.1016/0022-5096\(77\)90022-9](https://doi.org/10.1016/0022-5096(77)90022-9)
- Withers, P.J., 1989. The determination of the elastic field of an ellipsoidal inclusion in a transversely isotropic medium, and its relevance to composite materials. *Philosophical Magazine A* 59, 759–781. <https://doi.org/10.1080/01418618908209819>

## A Tensor algebra

## B Hill polarization tensor in elasticity

This section recalls some results about the calculation of the Hill polarization tensors related to a matrix of stiffness  $\mathbb{C}$  and an ellipsoid  $\mathcal{E}_A$  of equation

$$\underline{x} \in \mathcal{E}_A \quad \Leftrightarrow \quad \underline{x} \cdot ({}^t A \cdot A)^{-1} \cdot \underline{x} \leq 1$$

where  $A$  is an invertible second-order tensor so that  ${}^t A \cdot A$  is a positive definite symmetric tensor associated to 3 radii (eigenvalues  $a \geq b \geq c$  possibly written  $\rho_1 \geq \rho_2 \geq \rho_3$  for convenience) and 3 angles (orientation of the frame of eigenvectors  $\underline{e}_1, \underline{e}_2, \underline{e}_3$ )

$${}^t A \cdot A = a^2 \underline{e}_1 \otimes \underline{e}_1 + b^2 \underline{e}_2 \otimes \underline{e}_2 + c^2 \underline{e}_3 \otimes \underline{e}_3 = \sum_{i=1}^3 \rho_i \underline{e}_i \otimes \underline{e}_i \quad (\text{B.1})$$

### B.1 General expression

A general expression of the elastic polarization tensor is derived in (Willis, 1977) (see also (Mura, 1987))

$$\begin{aligned} \mathbb{P}(A, \mathbb{C}) &= \frac{1}{4\pi} \int_{\|\underline{\zeta}\|=1} (A^{-1} \cdot \underline{\zeta}) \overset{s}{\otimes} \left( (A^{-1} \cdot \underline{\zeta}) \cdot \mathbb{C} \cdot (A^{-1} \cdot \underline{\zeta}) \right)^{-1} \overset{s}{\otimes} (A^{-1} \cdot \underline{\zeta}) dS_{\underline{\zeta}} \\ &= \frac{\det A}{4\pi} \int_{\|\underline{\xi}\|=1} \frac{\underline{\xi} \overset{s}{\otimes} (\underline{\xi} \cdot \mathbb{C} \cdot \underline{\xi})^{-1} \overset{s}{\otimes} \underline{\xi}}{\|A \cdot \underline{\xi}\|^3} dS_{\underline{\xi}} \end{aligned} \quad (\text{B.2})$$

When  $\mathbb{C}$  is arbitrarily anisotropic, it is necessary to resort to numerical cubature to estimate  $\mathbb{P}$  as proposed in (Ghahremani, 1977), (Gavazzi and Lagoudas, 1990) or (Masson, 2008). However in some cases of anisotropy, analytical solutions are available ((Withers, 1989), (Barthélémy, 2020)). The case of isotropic matrix is particularly developed in the next section.

### B.2 Isotropic matrix

In this section, the matrix is assumed isotropic so that its stiffness tensor writes by means of a bulk  $k$  and shear  $\mu$  or Lamé  $\lambda$  and  $\mu$  moduli or even Young modulus  $E$  and Poisson ratio  $\nu$



with  $k = \frac{E}{3(1-2\nu)}$  and  $\mu = \frac{E}{2(1+\nu)}$ .

$$\begin{aligned} \mathbb{C} &= 3k\mathbb{J} + 2\mu\mathbb{K} = 3\lambda\mathbb{I} + 2\mu\mathbb{K} \\ \text{with } J_{ijkl} &= \frac{\delta_{ij}\delta_{kl}}{3}, I_{ijkl} = \frac{\delta_{ik}\delta_{jl} + \delta_{il}\delta_{jk}}{2} \text{ and } \mathbb{K} = \mathbb{I} - \mathbb{J} \end{aligned} \quad (\text{B.3})$$

Introducing Equation B.3 in Equation B.2 leads to after some algebra

$$\mathbb{P} = \frac{1}{\lambda + 2\mu}\mathbb{U} + \frac{1}{\mu}(\mathbb{V} - \mathbb{U})$$

where the tensors  $\mathbb{U}$  and  $\mathbb{V}$ , depending only on the ellipsoidal tensor  $\mathbf{A}$  of Equation B.1, are given by (see (Barthélemy, 2020))

$$\begin{aligned} \mathbb{U} &= \frac{\det \mathbf{A}}{4\pi} \int_{\|\underline{\xi}\|=1} \frac{\underline{\xi} \otimes \underline{\xi} \otimes \underline{\xi} \otimes \underline{\xi}}{\|\mathbf{A} \cdot \underline{\xi}\|^3} dS_{\underline{\xi}} \\ &= \frac{1}{4\pi} \int_{\|\underline{\zeta}\|=1} \frac{(\mathbf{A}^{-1} \cdot \underline{\zeta}) \otimes (\mathbf{A}^{-1} \cdot \underline{\zeta}) \otimes (\mathbf{A}^{-1} \cdot \underline{\zeta}) \otimes (\mathbf{A}^{-1} \cdot \underline{\zeta})}{\|\mathbf{A}^{-1} \cdot \underline{\zeta}\|^4} dS_{\underline{\zeta}} \end{aligned}$$

and

$$\begin{aligned} \mathbb{V} &= \frac{\det \mathbf{A}}{4\pi} \int_{\|\underline{\xi}\|=1} \frac{\underline{\xi}^s \otimes 1 \otimes \underline{\xi}^s}{\|\mathbf{A} \cdot \underline{\xi}\|^3} dS_{\underline{\xi}} \\ &= \frac{1}{4\pi} \int_{\|\underline{\zeta}\|=1} \frac{(\mathbf{A}^{-1} \cdot \underline{\zeta})^s \otimes 1 \otimes (\mathbf{A}^{-1} \cdot \underline{\zeta})^s}{\|\mathbf{A}^{-1} \cdot \underline{\zeta}\|^2} dS_{\underline{\zeta}} \end{aligned}$$

For an arbitrary ellipsoid defined by Equation B.1, the components of  $\mathbb{U}$  and  $\mathbb{V}$  write

$$\begin{aligned} U_{iiii} &= \frac{3(I_i - \rho_i^2 I_{ii})}{2} \quad \forall i \in \{1, 2, 3\} \\ U_{iijj} = U_{ijij} = U_{ijji} &= \frac{I_j - \rho_i^2 I_{ij}}{2} = \frac{I_i - \rho_j^2 I_{ij}}{2} \quad \forall i \neq j \in \{1, 2, 3\} \end{aligned}$$

and

$$\begin{aligned} V_{iiii} &= I_i \quad \forall i \in \{1, 2, 3\} \\ V_{ijij} = V_{ijji} &= \frac{I_i + I_j}{4} \quad \forall i \neq j \in \{1, 2, 3\} \end{aligned}$$

where the coefficients  $I_i$  and  $I_{ij}$  are given by (note that  $I_i$  and  $I_{ij}$  are adapted from those provided in (Kellogg, 1929) and (Eshelby, 1957): they differ by a factor of  $4\pi/3$  for  $I_{ij}$  with  $i \neq j$  and by  $4\pi$  for the others)

- if  $a > b > c$

$$\begin{aligned}
I_1 &= \frac{a b c}{(a^2 - b^2)\sqrt{a^2 - c^2}} (F - E) \\
I_3 &= \frac{a b c}{(b^2 - c^2)\sqrt{a^2 - c^2}} \left( \frac{b\sqrt{a^2 - c^2}}{a c} - E \right) \\
I_2 &= 1 - I_1 - I_3 \\
I_{ij} &= \frac{I_j - I_i}{\rho_i^2 - \rho_j^2} \quad \forall i \neq j \in \{1, 2, 3\} \\
I_{ii} &= \frac{1}{3} \left( \frac{1}{\rho_i^2} - \sum_{j \neq i} I_{ij} \right) \quad \forall i \in \{1, 2, 3\}
\end{aligned}$$

where  $F = F(\theta, \kappa)$  and  $E = E(\theta, \kappa)$  are respectively the elliptic integrals of the first and second kinds (see (Abramowitz and Stegun, 1972)) of amplitude and parameter

$$\theta = \arcsin \sqrt{1 - \frac{c^2}{a^2}} \quad ; \quad \kappa = \sqrt{\frac{a^2 - b^2}{a^2 - c^2}}$$

- if  $a > b = c$  (prolate spheroid)

$$\begin{aligned}
I_2 = I_3 &= a \frac{a\sqrt{a^2 - c^2} - c^2 \operatorname{arccosh}(a/c)}{2(a^2 - c^2)^{3/2}} \\
I_1 &= 1 - 2 I_3 \\
I_{1i} = I_{i1} &= \frac{I_i - I_1}{a^2 - \rho_i^2} \quad \forall i \in \{2, 3\} \\
I_{ij} &= \frac{1}{4} \left( \frac{1}{c^2} - I_{31} \right) \quad \forall i, j \in \{2, 3\} \\
I_{11} &= \frac{1}{3} \left( \frac{1}{a^2} - 2 I_{31} \right)
\end{aligned}$$

- if  $a = b > c$  (oblate spheroid)

$$\begin{aligned}
I_1 = I_2 &= c \frac{a^2 \arccos(c/a) - c\sqrt{a^2 - c^2}}{2(a^2 - c^2)^{3/2}} \\
I_3 &= 1 - 2 I_1 \\
I_{3i} = I_{i3} &= \frac{I_3 - I_i}{\rho_i^2 - c^2} \quad \forall i \in \{1, 2\} \\
I_{ij} &= \frac{1}{4} \left( \frac{1}{a^2} - I_{31} \right) \quad \forall i, j \in \{1, 2\} \\
I_{33} &= \frac{1}{3} \left( \frac{1}{c^2} - 2 I_{31} \right)
\end{aligned}$$

- if  $a = b = c$  (sphere)

$$I_1 = I_2 = I_3 = \frac{1}{3}$$

$$I_{ij} = \frac{1}{5a^2} \quad \forall i, j \in \{1, 2, 3\}$$

In this last case of spherical inclusion ( $A = 1$ ),  $\mathbb{U}$  and  $\mathbb{V}$  are simply decomposed as

$$\mathbb{U} = \frac{1}{3}\mathbb{J} + \frac{2}{15}\mathbb{K} \quad \text{and} \quad \mathbb{V} = \frac{1}{3}\mathbb{I}$$

### B.3 Case of cracks

The case of cracks corresponds to ellipsoids for which the smallest radius is very small compared to the two others, in other words the characteristic tensor  $A$  Equation B.1 can be written here

$$A = \underline{\ell} \otimes \underline{\ell} + \eta \underline{m} \otimes \underline{m} + \omega \underline{n} \otimes \underline{n} \quad \text{with} \quad \eta = \frac{b}{a} \quad \text{and} \quad \omega = \frac{c}{a}$$

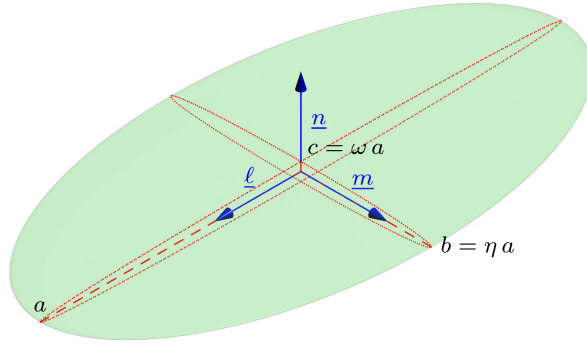


Figure B.1: Ellipsoidal crack

In the case of cracks, it is useful to introduce the second Hill polarization tensor defined as

$$\mathbb{Q} = \mathbb{C} - \mathbb{C} : \mathbb{P} : \mathbb{C}$$

and in particular  $\lim_{\omega \rightarrow 0} \omega \mathbb{Q}^{-1}$  in which it is recalled that  $\mathbb{P}$  and thus  $\mathbb{Q}$  depend on  $\omega$  such that the components  $Q_{nijk}$  (with  $n$  corresponding to the crack normal) behave as  $1/\omega$  when  $\omega$  tends towards 0. The analytical expressions of this limit are fully detailed in (Barthélémy et al., 2021) which recalls in particular that  $\mathbb{L}$  actually derives from a symmetric second-order tensor  $B$  as

$$\mathbb{L} = \lim_{\omega \rightarrow 0} \omega \mathbb{Q}^{-1} = \frac{3}{4} \underline{n}^s \otimes B \otimes \underline{n}^s \quad (\text{B.4})$$

For an arbitrarily anisotropic matrix, an algorithm allowing to estimate the limit Equation B.4 is proposed in (Barthélemy, 2009) whereas in the isotropic case B writes

$$\mathbf{B} = B_{nn} \underline{n} \otimes \underline{n} + B_{mm} \underline{m} \otimes \underline{m} + B_{\ell\ell} \underline{\ell} \otimes \underline{\ell}$$

with

$$\begin{aligned} B_{nn} &= \frac{8\eta(1-\nu^2)}{3E} \frac{1}{\mathcal{E}_\eta} \\ B_{mm} &= \frac{8\eta(1-\nu^2)}{3E} \frac{1-\eta^2}{(1-(1-\nu)\eta^2)\mathcal{E}_\eta - \nu\eta^2\mathcal{K}_\eta} \\ B_{\ell\ell} &= \frac{8\eta(1-\nu^2)}{3E} \frac{1-\eta^2}{(1-\nu-\eta^2)\mathcal{E}_\eta + \nu\eta^2\mathcal{K}_\eta} \end{aligned}$$

where  $\mathcal{K}_\eta = \mathcal{K}(\sqrt{1-\eta^2})$  and  $\mathcal{E}_\eta = \mathcal{E}(\sqrt{1-\eta^2})$  are the complete elliptic integrals of respectively the first and second kind (see (Abramowitz and Stegun, 1972)). If the crack is circular, the components of B become

$$B_{nn} = \frac{16(1-\nu^2)}{3\pi E} \quad ; \quad B_{mm} = B_{\ell\ell} = \frac{B_{nn}}{1-\nu/2}$$

## B.4 Application of Hill calculation

```
import numpy as np
from echoes import *
import matplotlib.pyplot as plt
```

### B.4.1 Definition of the matrix tensor

```
C = stiff_Enu(1.,0.2) ; print(C)
```

```
Order 4 ISO tensor | Param(size=2)=[ 1.66667 0.833333 ] | Angles(size=0)=[ ]
[ 1.11111 0.277778 0.277778 0 0 0
  0.277778 1.11111 0.277778 0 0 0
  0.277778 0.277778 1.11111 0 0 0
  0 0 0 0.833333 0 0
  0 0 0 0 0.833333 0
  0 0 0 0 0 0.833333 ]
```

### B.4.2 Calculation of the crack compliance $\mathbb{L} = \lim_{\omega \rightarrow 0} \omega \mathbb{Q}^{-1}$

Note that in *Echoes* it is necessary to provide an aspect ratio  $\omega$  for the crack even if the crack compliance is actually calculated as a limit (not depending on  $\omega$ )

```
ω = 1.e-4
L = crack_compliance(spheroidal(ω), C) ; print(L)
```

```
[[0.      0.      0.      0.      0.      0.      ]
 [0.      0.      0.      0.      0.      0.      ]
 [0.      0.      1.22230996 0.      0.      0.      ]
 [0.      0.      0.      0.67906109 0.      0.      ]
 [0.      0.      0.      0.      0.67906109 0.      ]
 [0.      0.      0.      0.      0.      0.      ]]
```

### B.4.3 Checking the aspect ratio for which $\omega \mathbb{Q}^{-1} \approx \lim_{\omega \rightarrow 0} \omega \mathbb{Q}^{-1}$ is acceptable

```
tw = np.logspace(-5,1,20)
tabδ = []
for ω in tw:
    Q = hill_dual(spheroidal(ω), C)
    Lω = ω*np.linalg.inv(Q)
    δL = np.linalg.norm(Lω-L)/np.linalg.norm(L)
    tabδ.append(δL)
plt.figure(figsize=(8,3))
plt.loglog(tw,tabδ,'+-')
plt.xlabel(r"$\omega$")
plt.ylabel(r"$\frac{||\mathbb{L}-\omega\mathbb{Q}^{-1}||}{||\mathbb{L}||}$")
plt.grid(True,which='both')
plt.show()
```

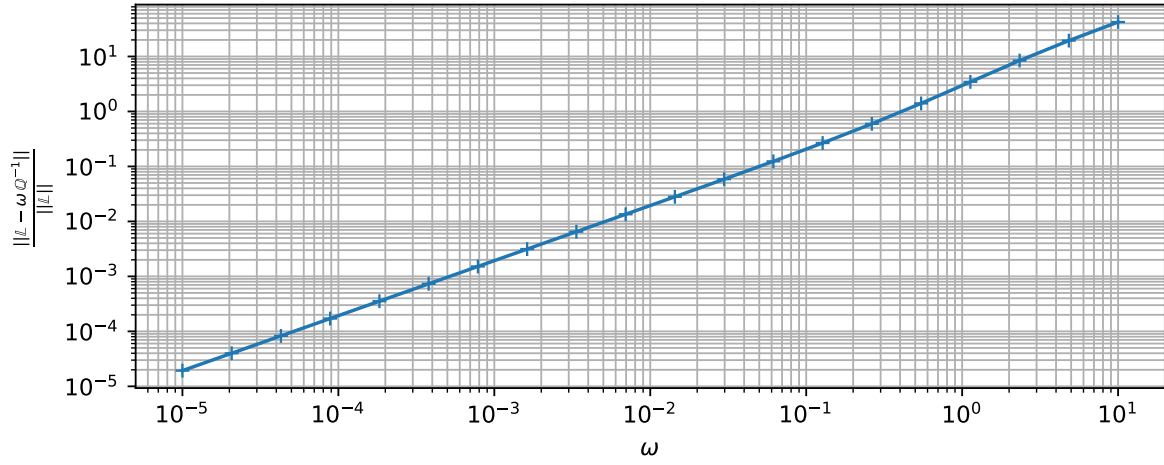


Figure B.2: Influence of the aspect ratio on the contribution tensor

## **C Hill polarization tensor in conductivity**